Using Sound Diffraction to Determine the Seabed Slope

Vincent Creuze, Bruno Jouvencel, Philippe Baccou

Using Sound Diffraction to Determine the Seabed Slope

V. Creuze, B. Jouvencel, P. Baccou

Laboratoire d'Informatique, de Robotique et de Microélectronique de Montpellier
LIRMM / CNRS, Université Montpellier II – UMR 5506
161 rue Ada, 34392 Montpellier CX 5, France
research.creuze@laposte.net, jouvencel@lirmm.fr, philippe.baccou@wanadoo.fr

***Abstract* - Navigation of autonomous underwater vehicles (A.U.V.) in very shallow waters implies acoustic detection. In single beam sonar systems, sound emitted by ultrasonic transducers is diffracted and secondary lobes appear. Considering the sea bottom's backscattering properties, secondary lobes can be used to enhance knowledge of seabed features such as slope, and marked variations. In this paper, we firstly consider characteristics of electro-acoustic transducers and study the resulting acoustic diffraction. Then, we introduce a new method aiming to extract seabed features from the received acoustic echo. Thus single beam sonar systems can be used for bottom tracking purposes. We present the results of our simulations and experimental validation.**

***Index Terms* – Acoustic detection, acoustic diffraction, bottom tracking, Autonomous Underwater Vehicles.**

I INTRODUCTION

For some years, Autonomous Underwater Vehicles (A.U.V.) have been substantially developed. Due to industrial and scientific requirements, the necessity of navigating in very shallow water has emerged. And then, features like positioning [1][2], obstacle avoidance [3][4], bottom tracking [5], and target characteristics [6] have been studied.

Acoustic detection of the environment is achieved through multi-beam forward looking sonar, lateral sonar, and now synthetic and interferometric sonar systems.

Many of these tasks require sophisticated equipment whose size, weight, and electrical consumption can be damaging to the vehicle's autonomy and its live load. This point is particularly critical for very small AUVs, like TAIPAN [10] our laboratory's prototype.

For bottom tracking applications such as survey or video imaging another approach can be studied. In fact, with single beam acoustic emitters, the emitted acoustic wave is diffracted. Features of this diffracted beam can be computed by using emitter dimensions, sound speed in water, and signal frequency.

Moreover, combining diffraction of the emitted signal with backscattering properties of the bottom allows us to work out data that is traditionally not obtained with single beam acoustic systems: bottom slope, and significant bottom variations such as underwater cliffs.

In this paper, we present a new method of seabed detection based on the use of a single electro-acoustic transducer (sounder). This method uses both acoustic diffraction and bottom backscattering coefficients.

Firstly, we present the acoustic sensor and the beam features due to diffraction. We also detail the bottom backscattering properties. In the second part, we explain the method, which is used to treat the acoustic echo received by the sensor. The last part consists in the presentation of simulated and experimental results.

II UNDERWATER SOUND THEORY

A. Assumptions

We consider an autonomous underwater vehicle fitted with a single electro acoustic transducer. The angle of orientation between transducer axis and vehicle axis is called ψ. The pitch angle of the vehicle is called ζ. The angle between seabed and the line of sight of the transducer is called ξ (Fig. 1). The bottom slope is defined as the angle between seabed and the horizontal plane.

The emitted signal is a sine pulse whose frequency is 200kHz. The transmit pulse length is called τ.

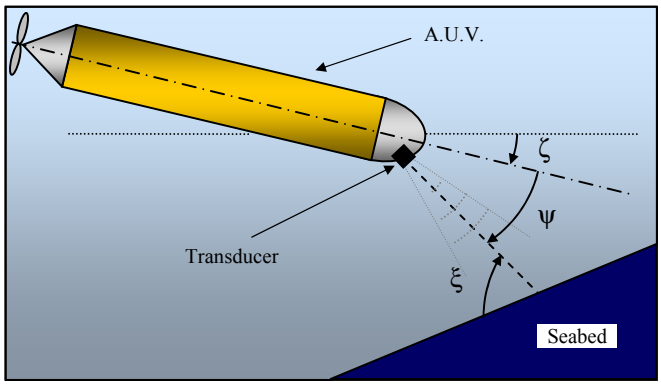

Fig. 1. The AUV and its transducer

B. Sound diffraction

When the aperture radius of the transducer is not very large (r_c < 15mm) in comparison with the wavelength (λ = 7.5mm), diffraction must be taken into account in the estimation of beam geometry.

For distances R bigger than λ / r_c (Fraunhofer zone) one can determine the beam geometry by application of the Huygens-Fresnel principle.

Sound intensity $I(R,\theta)$ at range R and angular deviation θ from the line-of-sight of the transducer is given by equation (1).

$$I(R,\theta) = I_o(R)\left(\frac{2J_1(2\pi f\frac{r_c}{c}\tan\theta)}{2\pi f\frac{r_c}{c}\tan\theta}\right)^2 \quad (1)$$

where $J_1(\ )$ is the Bessel function of first order, f is the frequency, r_C is the aperture radius of the transducer, c is sound speed, and $I_o(R)$ is the sound intensity at range R on the beam axis [7]. $I_o(R)$ depends on transmission loss and will be detailed in the next paragraph. The pattern obtained is also called the Airy diffraction pattern.

Angular attenuation of intensity (in dB) is called $Airy(\theta)$ and is given by:

$$Airy(\theta) = 10\log\left(\frac{2J_1(2\pi f\frac{r_c}{c}\tan\theta)}{2\pi f\frac{r_c}{c}\tan\theta}\right)^2 \quad (2)$$

Polar representation of intensity attenuation in decibels gives us the directivity diagram of the transducer, which shows us clearly the main lobe and two secondary lobes (Fig. 2). Attenuation of the sound intensity level is approximately 40 dB for the two secondary lobes (Fig. 3).

C. *Transmission loss*

The transmission loss (TL) consists of two parts, one due to spherical spreading, the other due to absorption loss in the water (3).

$$TL = 10\log R^2 + \alpha \,.\, 10^{-3} \,.\, R \quad (3)$$

where R is the range in meters, and α the absorption coefficient (in dB/km) and is related to the square of frequency [8].

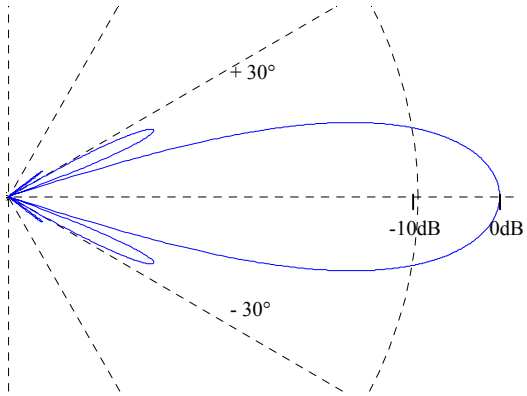

Fig. 2. Directivity of transducer

D. *Backscattering*

Once it has reached the seabed, the acoustic wave will be partially backscattered. The backscattering coefficient, BS, varies with the incidence angle φ (Fig.4) and is given in dB/m². So, backscattered intensity will depend both on incidence angle but also on the extent of the seabed area which contributes to the backscattered signal.

For incidence angles larger than about 25° a good approximation of backscattering coefficient BS is given by Lambert's law (4) [9].

$$BS = BS_o + 20\log(\cos\varphi_i) \quad (4)$$

where BS_o is a constant coefficient depending on seabed characteristics, and φ_i is the incidence angle.

For incidence angles smaller than 25° one can approximate backscattering coefficient BS by :

$$BS = BS_N + \frac{\varphi_i}{\varphi_o}\,(BS_o - BS_N + 20\log(\cos\varphi_o)) \quad (5)$$

where BS_N is the backscattering coefficient for normal incidence, BS_o is the backscattering coefficient used in Lambert's law (4), φ_o is the transition angle (=25°), and φ_i is the incidence angle.

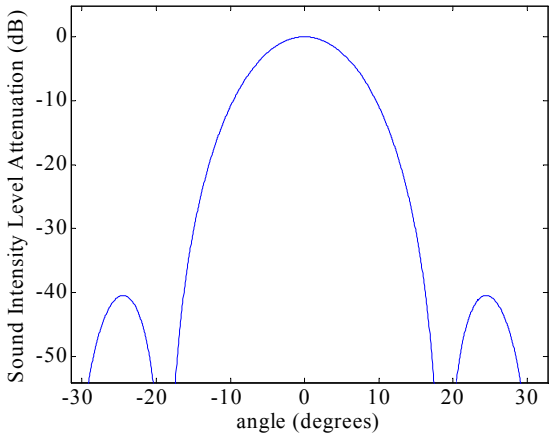

Fig. 3. Attenuation of sound intensity (in dB)

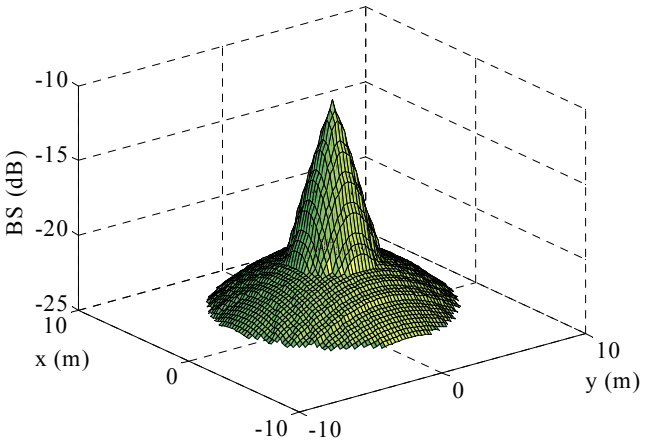

Fig. 4. Backscattering coefficient (in dB)

In order to take into account the extent of the seabed area which contributes to the backscattered signal, *BS* has to be normalized. The normalized backscattering coefficient is called *BTS* and is given by :

$$BTS = BS + 10\log(\sigma) \qquad (6)$$

where σ represents the extent of the seabed area which contributes to the backscattered signal and depends on beam geometry and transmit pulse length.

E. Total attenuation

In order to calculate sound intensity of the signal backscattered by each seabed part, we determine *H*, the total attenuation per unit area (7) by adding dB values of attenuation due to diffraction (2), two-way transmission loss (3), and backscattering (6).

$$H = Airy - 2\,TL + BTS \qquad (7)$$

III PROCESSING THE RECEIVED SIGNAL

A. Received sound pressure

Considering §II, sound pressure $s(t)$ of the backscattered signal is given by:

$$s(t) = \iint_S e\left(t - \Delta t(x,y)\right) 10^{\frac{H(x,y)}{20}}\, dx\, dy \qquad (8)$$

where $e(t)$ is the sound pressure pulse emitted by the transducer, S is the extent of the seabed area which contributes to the echo (defined by the beam geometry), (x,y) are coordinates on seabed, $\Delta t(x,y)$ is the delay defined by:

$$\Delta t(x,y) = 2\,\frac{R(x,y)}{c} \qquad (9)$$

and $H(x,y)$ is the attenuation (in dB):

$$H(x,y) = Airy(x,y) - 2\,TL(x,y) + BTS(x,y) \qquad (10)$$

B. Bottom slope

Due to the orientation of the transducer (Fig. 5), backscattering level *BTS* is lower for main lobe signal than for secondary lobe. The same effect occurs for transmission loss *TL*. Consequently, in spite of Fraunhofer attenuation, global attenuation level *H* makes secondary lobe echo level significant in comparison with main lobe echo level (Fig. 6). Thus, the backscattered acoustic signal is made of two peaks corresponding firstly to the secondary lobe echo and secondly to the main lobe echo (Fig. 7.)

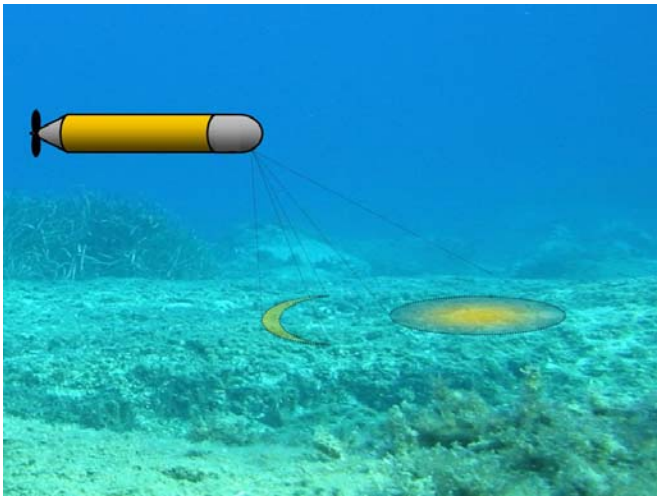

Fig. 5. Main and secondary lobes of the acoustic beam

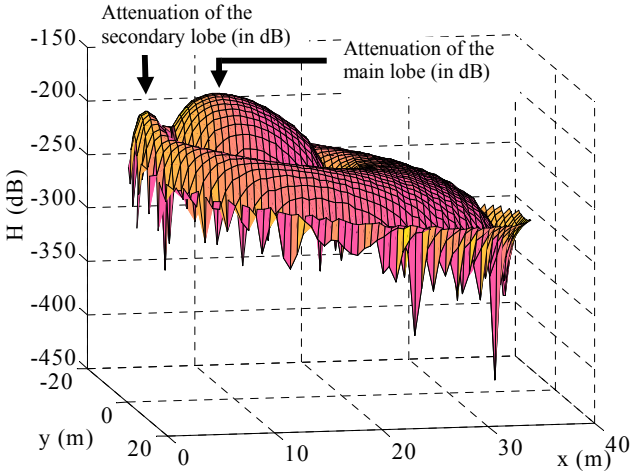

Fig. 6. Global attenuation of acoustic beam

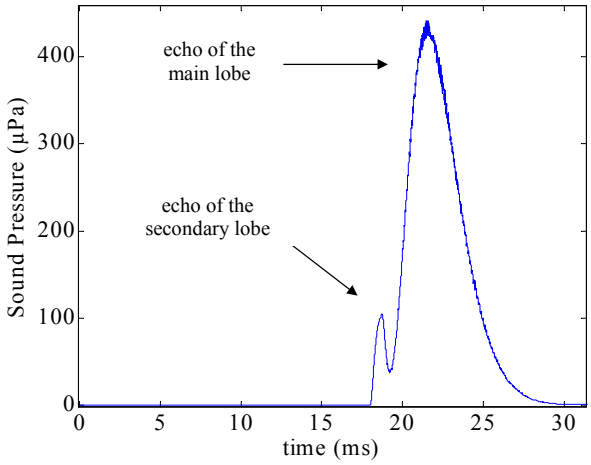

Fig. 7. Backscattered acoustic signal

Bottom slope can be computed by measuring the time between the two peaks corresponding to secondary and main lobes of the acoustic beam. It has to be noticed that pressure peaks correspond to main and secondary lobes only when angular decrease of the Airy attenuation is larger than angular decrease of backscattering coefficients.

This assumption depends on BS_o and BS_N backscattering coefficients but is verified in most of cases. Under these conditions, one can demonstrate that ξ the angle between the seabed and the line of sight of the transducer can be expressed as (11) :

$$\xi = \cos^{-1}\left(\frac{t_p - t_s\cos\theta_s}{\sqrt{t_p^2 + t_s^2 - 2t_p t_s\cos\theta_s}}\right) \quad (11)$$

where t_p and t_s are respectively the instants of occurrence of peaks of sound intensity due to main and secondary lobes, and θ_S is the angle between axes of main and secondary lobes and is given by the theory of diffraction as to be:

$$\theta_S = \text{atan}(0.848\,\frac{\lambda}{r_c}) \quad (12)$$

where λ is the sound wavelength (7mm) and r_C is the aperture radius of the transducer. Then the seabed slope is simply given by:

$$slope = \xi - \psi - \zeta \quad (13)$$

where ξ is the angle between seabed and the line of sight of the transducer, ψ is the orientation angle of the transducer, and ζ is the pitch angle of the vehicle (Fig. 1).

IV SIMULATIONS AND EXPERIMENTATIONS

A. Simulations

Simulations have been conducted under Matlab™ environment. The seabed is represented by a grid whose mesh size is smaller than $c.\tau$, where c is the sound speed and τ is the transmit pulse length.

The sound pressure $p_{echo}(t)$ of the received echo is given by:

$$p_{echo}(t) = \sum_{ij} p_{emitted}\,(t - \Delta t_{ij}).10^{\frac{H_{ij}}{20}} \quad (14)$$

where $p_{emitted}$ is the emitted acoustic pressure at 1 meter along the line-of-sight of the transducer, (i,j) are coordinates in the seabed grid, H_{ij} is the attenuation (in dB), and Δt is given by (9).

In the following example, we have considered a transducer whose aperture diameter is 27 millimeters (r_c=13.5mm). The values of backscattering coefficients are: BS_o = -35dB and BS_N = -10dB. The transition angle of Lambert's law is $\varphi_o = 20°$. The angle of orientation between the axis of the transducer and the seabed is 50° and the water is 14 meters deep.

The results of simulations show clearly the presence of a secondary impact area due to diffraction (Fig. 8). For angles of orientation greater than 20°, backscattering properties of the seabed make the related secondary echoes non negligible. One can see that even if it is weak, the echo of the secondary lobe appears in the received acoustic signal (Fig. 9.a. and 9.b). This secondary lobe echo corresponds to the small peak of acoustic pressure that occurs at the beginning of the acoustic echo.

In this example, the delay between the first weak peak and the main peak of the signal is about 2.1 ms. Applying (11) with θ_s = 25.2°, t_p = 22.7ms, and t_s = 18.3ms, gives us ξ = 51.7°. The angle of orientation was set to 50°.

Other simulations have been conducted with different parameters and the liability of the results has not been affected.

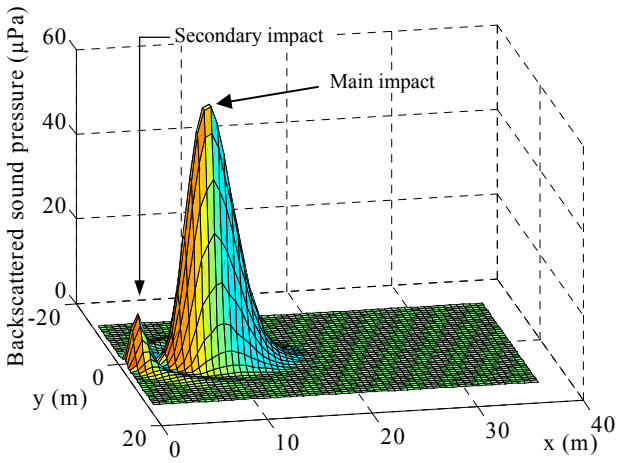

Fig. 8. Sound pressure backscattered by meshes of the seabed grid

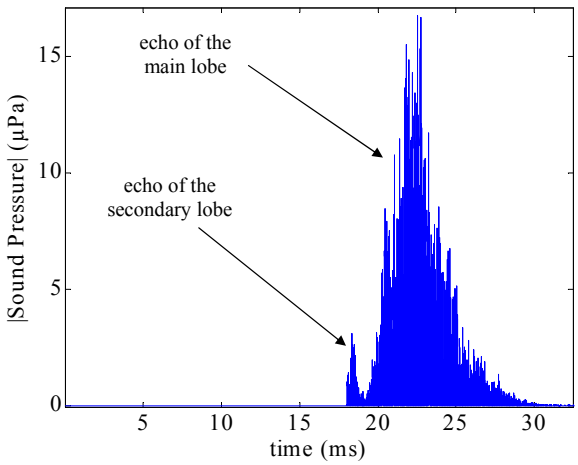

Fig. 9.a. Sound pressure of the acoustic echo

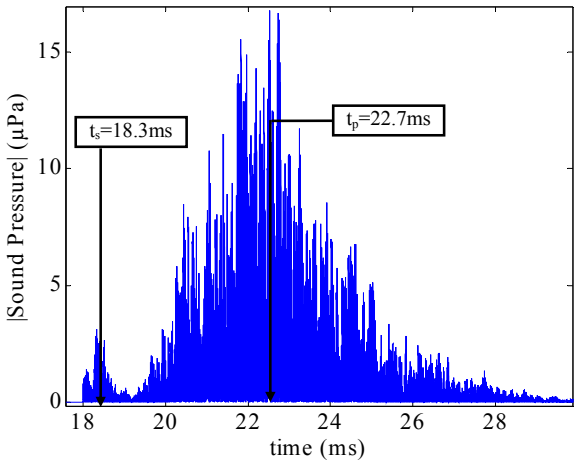

Fig. 9.b. Sound pressure of the acoustic echo (detail)

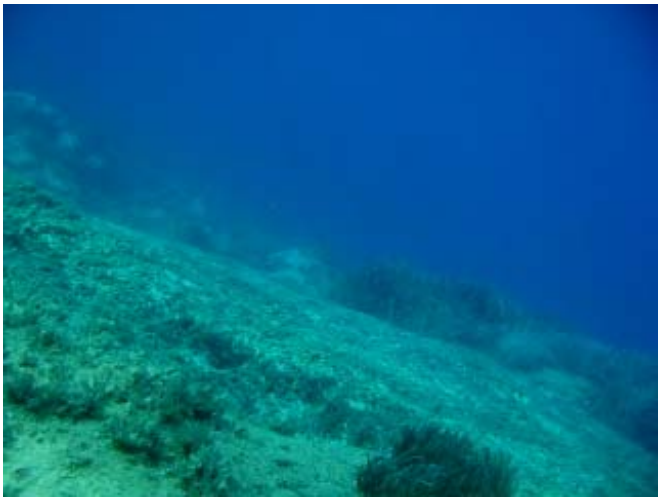

Fig. 10. Seabed where experimentation took place

B. Experimental device

In order to perform experimental validation, we have used one electro-acoustic transducer whose operating frequency is 200kHz. A specific electronic circuit has been designed. It is computer controlled and one can choose the transmit pulse length. A Time Varying Gain is applied to the backscattered signal so that it is at an optimum level for the 12 bits A/D converter. Then, the received signal is sent to the computer and processed.

C. Experimental results

Experimentation has been conducted in the Mediterranean. The seabed was mainly rocky (Fig. 10) and its slope was about 20°. The mean depth was 14 meters. Many angles of orientation of the transducer have been tested. In the following example the angle of orientation of the transducer is 30°, which corresponds to an angle of 50° between the seabed and the line-of-sight of the transducer.

On the measured acoustic echo (Fig. 11.a and 11.b) one can clearly see the first small peak due to backscattering of the secondary lobe of the acoustic beam. Applying (11) with $\theta_s = 21°$, $t_p = 22.6$ms, and $t_s = 18.6$ms, gives us $\xi = 51.8°$, which corresponds to the measured angle between the seabed and the line-of-sight of the transducer.

We have tested many other values of the angle of orientation between the seabed and the transducer. Comparing these angles of orientation with the ones computed by using (11) shows a good ability of our method to detect the seabed slope (Fig. 12).

For decreasing values of this angle, the detection of the small peak is no more possible as the backscattered acoustic energy weakens. This is due to the increasing value of the angle of incidence of the secondary beam which makes the backscattering coefficient smaller.

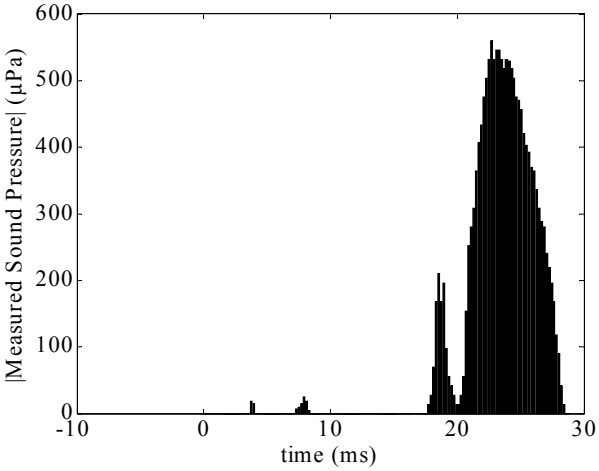

Fig. 11.a. Measured acoustic echo

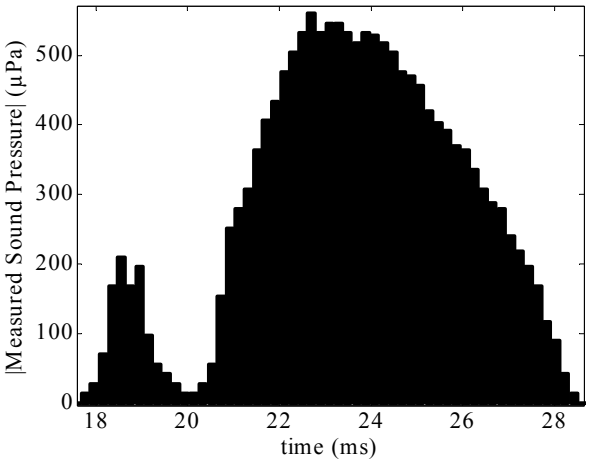

Fig. 11.b. Measured acoustic echo (detail)

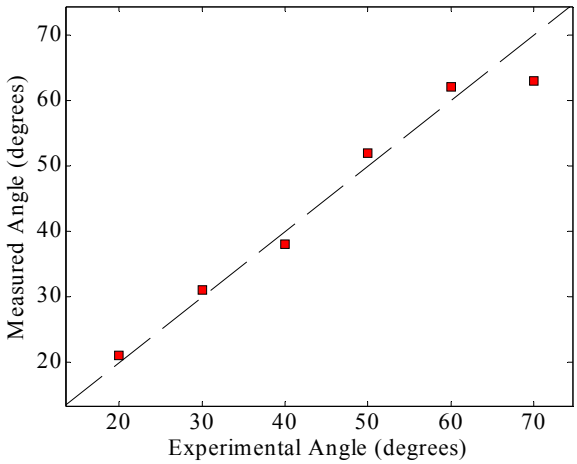

Fig. 12. True and computed angles of orientation

Conversely, for values bigger than 70°, the main beam becomes too wide to allow accurate peak detection. Moreover, as experiments have been conducted at small depth of immersion, for angles greater than 70° the upper secondary beam is reflected by the surface of the sea. This phenomenon has to be taken into account when the AUV navigates close to the surface but it will disappear as soon as the AUV will be closer to the bottom than to the surface.

We have also tested two other sizes of transducers. The obtained results show that diffraction is not significant enough for transducers whose diameter exceeds 3.5 cm. This is due to the ratio between the wavelength of the acoustic wave and the aperture diameter of the transducer.

V CONCLUSION

This paper describes how Fraunhofer diffraction can be used as an advantage in detection of the seabed slope. Detection capabilities of a single acoustic transducer can be increased when backscattering and Airy pattern are considered simultaneously. We have explained under which conditions, the secondary beam of the acoustic beam can give a significant echo and how this echo can be used to work out the seabed slope. Simulations have been conducted and their results have been validated by experimentation in the open sea. The designed device shows a good ability to determine the seabed slope and will soon be implemented on our new small AUV prototype "*Taipan 2"* (Fig. 13).

Presently, our research concerns the orientation of the transducer in order to get better performances of bottom tracking for AUV and we study different shaped transducers (rectangular) [11]. We also study how to combine the said acoustic properties with the DVZ concept [12] to achieve bottom tracking.

Fig. 13. The AUV Taipan 2

REFERENCES

[1] J.J. Leonard and H.F. Durrant-Whyte, "Directed Sonar Sensing for Mobile Robot Navigation," *ser. The Kluwer International Series in Engineering and Computer Science*, Norwell, MA: Kluwer, 1992.

[2] P. Baccou, B. Jouvencel, and V. Creuze, "Homing and Navigation Using One Transponder," *IEEE ICRA2002*, Washington D.C., May 2002.

[3] Y. Petillot, I. Tena Ruiz, and D. M. Lane, "Underwater Vehicle Obstacle Avoidance Using a Multi-Beam Forward Looking Sonar," *IEEE Journal of Oceanic Engineering*, Vol. 26, no. 2, pp. 240-251, April 2001.

[4] V. Creuze and B. Jouvencel, "Avoidance of Underwater Cliffs for Autonomous Underwater Vehicles," *IEEE IROS 2002*, Lausanne, Switzerland, pp. 793-798, October 2002.

[5] V.Creuze and B. Jouvencel, "Perception et suivi de fond pour véhicules autonomes sous-marins", *Traitement du Signal*, 2003 Vol. 20 no. 4, pp. 323-336, December 2003.

[6] J.R. Edwards, H. Schmidt, and K.D. LePage, "Bistatic Synthetic Aperture Target Detection and Imaging with an AUV," *IEEE Journal of Oceanic Engineering*, Vol. 26, no. 4, pp. 690-699, October 2001.

[7] A.D. Pierce, *Acoustics, an introduction to its physical principles and applications*, McGraw Hill, New-York, 1981.

[8] Robert J. Urick, *Principles of Underwater Sound*, Peninsula Publishing, 1983.

[9] X. Lurton, *An introduction to Underwater Acoustics – Principles and Applications*, Springer Praxis Books, 2003.

[10] J. Vaganay, B. Jouvencel, P. Lépinay, and R. Zapata, "Taipan, an AUV for very Shallow Water Applications," *WAC'98*, Anchorage, 1998.

[11] V. Creuze, B. Jouvencel, and P. Baccou, "3D-Bottom Tracking based on Acoustic Diffraction for Autonomous Underwater Vehicles," *IEEE ICAR 2005*, Seattle, Washington, July 2005.

[12] R. Zapata, P. Lépinay, "Collision Avoidance and Bottom Following of a Torpedo-like Vehicle," *MTS/IEEE OCEANS96*, Fort Lauderdale, Florida, September 1996.